

Establishment of Kinetic Zone Diagrams via Simulated Linear Sweep Voltammograms for Soluble-Insoluble Systems

Imene Atek, Abed M. Affoune, Hubert Girault, Pekka Peljo

Abstract—Due to the need for a rigorous mathematical model that can help to estimate kinetic properties for soluble-insoluble systems, through voltammetric experiments, a Nicholson Semi Analytical Approach was used in this work for modeling and prediction of theoretical linear sweep voltammetry responses for reversible, quasi reversible or irreversible electron transfer reactions. The redox system of interest is a one-step metal electrodeposition process. A rigorous analysis of simulated linear scan voltammetric responses following variation of dimensionless factors, the rate constant and charge transfer coefficients in a broad range was studied and presented in the form of the so called kinetic zones diagrams. These kinetic diagrams were divided into three kinetics zones. Interpreting these zones leads to empirical mathematical models which can allow the experimenter to determine electrodeposition reactions kinetics whatever the degree of reversibility. The validity of the obtained results was tested and an excellent experiment–theory agreement has been showed.

Keywords—Electrodeposition, kinetics diagrams, modeling, voltammetry.

I. INTRODUCTION

LINEAR sweep voltammetry (LSV) is among well-known electro-analysis methods that played a great role to obtain a clear view about kinetics, thermodynamics and mechanisms of electrode reactions [1]-[3]. The technique consists to measure the electrons flow through an electrochemical system after applying linear sweep signals in time to an electrode. The essential LSV information for electrode reactions is generally registered as a peak in the current signal.

It has become widely accepted that, a simple visual inspection of typical voltammetric peaks is helpful, but it is often not enough to probe the physics and chemistry at the electrode-electrolyte interface. However, to overcome this issue, several simulation approaches have been employed to predict how an electrochemical system will respond under

voltammetric conditions [4].

Electrochemical systems, with soluble-soluble, insoluble-soluble redox couples, were extensively studied [5]-[7] through voltammetry techniques and several general mathematical models describing LSV responses for these systems under different conditions are available. While there have been relatively few attempts to investigate theoretical LSV responses in the case of soluble-insoluble phase transitions and any general equation models exist for this systems especially under quasi reversible conditions [5], [6].

In this paper, we extend the work in [8] to the problem of LSV, case of metal deposition reactions. We use a semi analytical approach. We begin by deriving an equivalent expression to the current and then show the characteristics of LSV responses for reversible, quasi-reversible and irreversible cases. And finally we provide to experimentalist a general strategy to extract directly the kinetic parameters from LSV data whatever the degree of the reversibility.

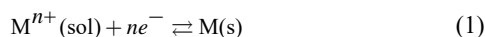
II. LSV EXPERIMENT PROTOCOL

For LSV experiment, the system of the reduction of Cu(I) in organic solution was studied, a copper disk of 2 mm diameter was used.

The electrolyte consisted of a mixture of given concentrations of $[\text{Cu}(\text{CH}_3\text{CN})_4]\text{BF}_4$ as a copper source, 100 mM tetraethylammonium tetrafluoroborate (TEABF4) as a supporting electrolyte, and acetonitrile as a solvent. Further experimental conditions used in this paper are given in [7].

III. EQUATION GOVERNING THE SYSTEM

In the present work, our attention focused on single step electrodeposition reaction. Thus, a soluble-insoluble system of metallic ions Mn^+ and metal M couple could be represented as:



Upon neglecting migration and convection contribution, the problem of the mass transport of metallic cations in Cartesian coordinates can be described with the Fick's differential law:

$$\frac{\partial C_{\text{M}^{n+}}(x,t)}{\partial t} = D_{\text{M}^{n+}} \frac{\partial^2 C_{\text{M}^{n+}}(x,t)}{\partial x^2} \quad (2)$$

It's necessary to define a set of initial and boundary conditions

I. Atek and A. M. Affoune are with Laboratoire d'Analyses Industrielles et Génie des Matériaux, Département de Génie des Procédés, Faculté des Sciences et de la Technologie, Université 8 Mai 1945 Guelma, BP 401, Guelma 24000, Algeria (e-mail: atek.imene@univ-guelma.dz, affoune.abedmohamed@univ-guelma.dz).

H. Girault is with Laboratoire d'Electrochimie Physique et Analytique, École Polytechnique Fédérale de Lausanne, EPFL Valais Wallis, Rue de l'Industrie 17, Case Postale 440, CH-1951 Sion, Switzerland (e-mail: hubert.girault@epfl.ch).

P. Peljo is with Research group of Physical Electrochemistry and Electrochemical Physics, Department of Chemistry and Materials Science, Aalto University PO Box 16100, 00076 Aalto, Finland (e-mail: pekka.peljo@aalto.fi).

to solve the above differential partial equation. These conditions are as:

$$t = 0, C_{M^{n+}}(x, 0) = C_{M^{n+}}^* \quad (3)$$

$$x \rightarrow \infty, C_{M^{n+}}(\infty, t) = C_{M^{n+}}^* \quad (4)$$

$$x \rightarrow 0, \frac{I(t)}{nFA} = -D_{M^{n+}} \left[\frac{\partial C_{M^{n+}}(x, t)}{\partial x} \right]_{x=0} \quad (5)$$

Equation (1) is assumed to be a simple charge transfer controlled reaction, so that the electrochemical kinetic in the present paper is described by Butler-Volmer equations that links the variables for current, electrode potential and concentrations as:

$$I(t) = nFAk^0 \left[C_M(0, t) \exp\left(\frac{(1-\alpha)nF}{RT}(E(t) - E^0)\right) - C_{M^{n+}}(0, t) \exp\left(\frac{-\alpha nF}{RT}(E(t) - E^0)\right) \right] \quad (6)$$

The electrode potential was swept in the negative direction:

$$E(t) = E_i - vt \quad (7)$$

where v is the scan rate and t is the time.

IV. COMPUTATION

We solved the coupled electrochemistry and mass transport system described by (2)-(7), using the semi-analytical method. We employed a four-step approach for solving this: first, we solved the ion transport problem by Laplace transformation, then substituted the solution into Butler-Volmer relation, converted the LSV parameters into a non-dimensional form as:

The dimensionless initial potential is expressed as follows:

$$Init = \frac{nF}{RT}(E_i - E^0) \quad (8)$$

The Dimensionless applied potential:

$$\Phi = \frac{nF}{RT}(E(t) - E^0) = Init - \sigma t \quad (9)$$

The dimensionless scan rate:

$$\sigma = \frac{nF}{RT}v \quad (10)$$

The dimensionless kinetic rate constant [5]:

$$\omega = \frac{k^0}{\theta^\alpha \left(\pi D \frac{nF}{RT} v \right)^{1/2}} \quad (11)$$

and we finally solve the resulted equations system numerically, and thus, we define the final solution as:

$$I(t) = nFA C_{M^{n+}}^* (\pi D_{M^{n+}})^{1/2} \left(\frac{nFv}{RT} \right)^{1/2} \Psi(\sigma t) \quad (12)$$

V. RESULTS

A. Qualitative Analysis of Calculated Voltammograms

1. Reversible Charge Transfer

In Fig. 1, we present our first results for the case of reversible charge transfer in which the dimensionless peak current is equal to -0.610 , and we compared it with the analytic solution of Berzin and Delahay [8], an excellent agreement is found between the two for the values of the dimensionless parameters $\omega = 10^4$ and $\alpha = 0.5$.

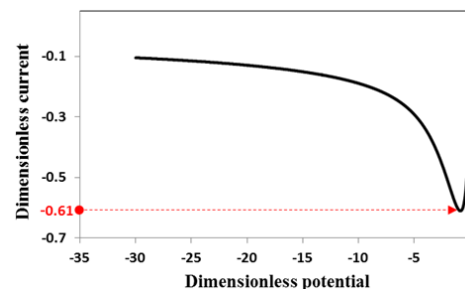


Fig. 1 Linear sweep voltammogram simulated for fully reversible charge transfer ($\omega = 10^4$ and $\alpha = 0.5$)

2. Quasi-Reversible Charge Transfer

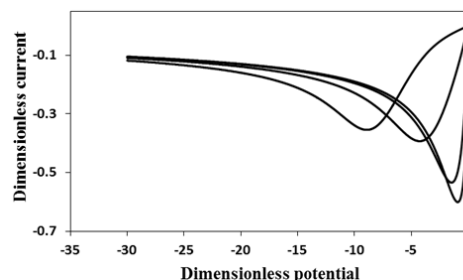


Fig.2 Linear sweep voltammograms for quasi-reversible charge transfer produced for (from right to left) $\omega = 100, 10, 1.0$ and 0.1 and $\alpha = 0.5$

Now we consider the case of quasi-reversible charge transfer for which there is no known solution. We varied the dimensionless rate constant, ω , in the range of $[100-0.1]$ with α equal to 0.5 . These are the same parameter values as used in [9]. The results produced are shown in Fig. 2, in which we remark that a decrease in the rate constant leads to a diminution in the height of the peak current, an increase in the

peak width, and a displacement of the dimensionless peak potential towards more negative values.

3. Irreversible Charge Transfer

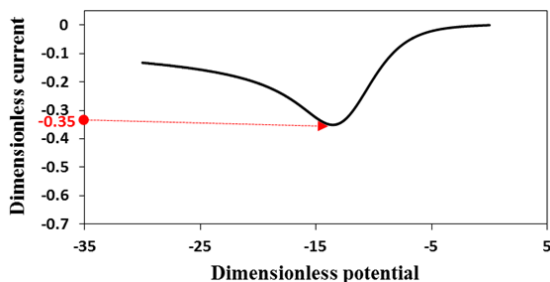


Fig. 3 Linear sweep voltammograms for totally irreversible soluble-insoluble system with $\omega = 10^{-3}$ and $\alpha = 0.5$

For a value of the rate constant equal to 10^{-3} , the dimensionless peak current passes through a maximum of 0.350, in absolute value, and the LSV responses exhibits an irreversible character.

B. Quantitative Analysis of Calculated Voltammograms

1. Kinetics Zone Diagrams

In order to provide a general, simple and direct strategy to diagnose the type of metal deposition reactions and to calculate their kinetic parameters, we have constructed three-dimensional diagram. In each diagram we show how the variation of both; the dimensionless kinetic rate (ω) and the electron transfer coefficient α shift the system from reversible to irreversible zone through controlling the corresponding changes, first in the magnitude of the peak current (Fig. 4 (a)), after in the peak shape (Fig. 4 (b)) and finally in the peak position (Fig. 4 (c)).

For $\log \omega \geq 3$, we remark that all peak parameters are independent of the values of the charge transfer coefficient and the dimensionless kinetic rate constant, so that, from this value, we define the limits of reversible deposition reactions zone. In the regions where $-3 < \log \omega < 3$, marked changes in the various peak parameters as a function of both $\log \omega$ and α are produced, so that the system approaches the quasi-reversible limit according to Matsuda and Ayab diagnostic criteria [9]. While, in the case of small values of rate constant ($\log \omega \leq -3$), the soluble insoluble system responds in irreversible manner, characteristics of these are the magnitude of peak current and half peak width takes specific values at specific values of α while the peak potential continues to decrease linearly as the function of decreasing the rate constant.

2. Mathematic Models

As Figs. 4 (a) and (b) are sigmoidal in shapes, fitting data yield to the following general models:

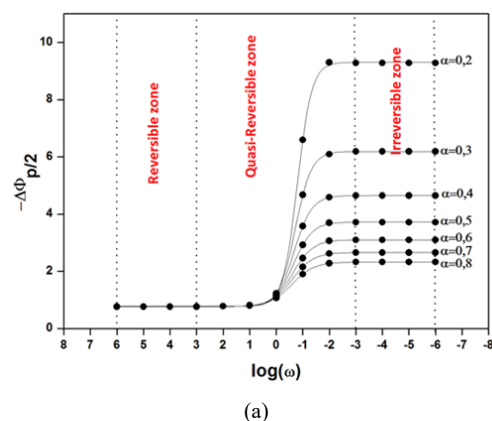
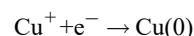
$$\frac{\psi_p}{(\psi_p)_{rev}} = 1 + \frac{(0.811\alpha^{0.5} - 1)}{1 + \exp\left[\frac{X - (-0.528\alpha - 0.099)}{0.477\alpha^{0.248}}\right]} \quad (12)$$

$$-\Delta\Phi_{p/2} = 0.770 + \frac{(1.857\alpha^{-1} - 0.770)}{1 + \exp\left[\frac{X + (0.557\alpha^{-0.216})}{0.445\alpha^{0.316}}\right]} \quad (13)$$

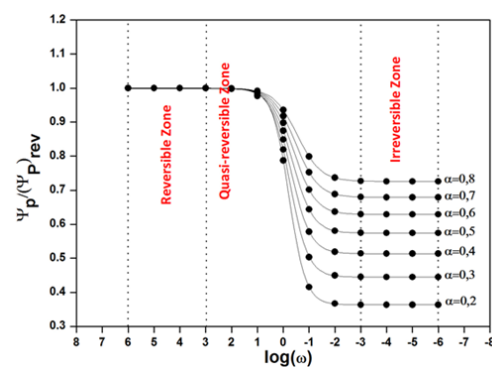
Each of these fit models enables voltammetric quantification of the electrode kinetics from simple examination of an experimental linear sweep voltammograms whatever the degree of reversibility, provided that the value of α is known or can be estimated accurately. Note that the diagram represented in Fig. 4 (c) was well fitted by [5] to linear models and this is beyond of this paper.

C. Validation

The Cu deposition electrochemical system is chosen to compare with our theoretical models. According to [10], the Cu system is a one step, one-electron transfer reaction:



(a)



(b)

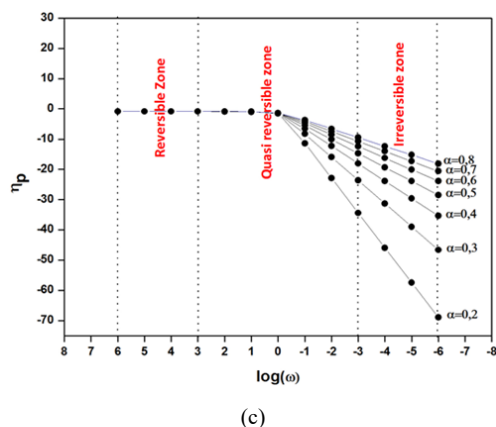


Fig. 4 Kinetic zone diagrams: (a) variation of the peak current ratio, $\Psi_p / (\Psi_p)_{rev}$ as the function of the dimensionless rate constant where $(\Psi_p)_{rev}$ is the reversible dimensionless peak current; (b) variation of the peak shape through the half peak width changes, $\Delta\Phi_{p/2} = \frac{nF}{RT}(E_p - E_{p/2})$, as the function of the rate constant; (c) variation of the cathodic peak position $\eta_p = \frac{nF}{RT}(E_p - E_{eq})$, as a function of rate constant

Fig. 5 (a) illustrates linear sweep voltammogram curves recorded at various scan rates for electrodeposition of Cu(I) on Cu disc electrode from 10.25 mM of tetrakis(acetonitrile)copper(I) tetrafluoroborate in acetonitrile. As we increase the scan rate, v , from 0.01 to 2 V/s, we observe a general increase in the magnitude of the LSV responses and slight peak potential shift.

In the present paper, the diffusion coefficient was calculated by the direct application of semi-integration technique and the obtained value is in good agreement with the values previously reported in literature [11], while the charge transfer coefficient was determined by application of Tafel analysis on the typical voltammetric current recorded at 100 mV/s, and then the rate constant was calculated using models presented by (12) and (13), which indicated a quasi-reversible behavior. Thus to demonstrate the accuracy of our models, an example of voltammogram (Fig. 5 (b)) was simulated by using the calculated parameters illustrated in Table I. Likewise, The kinetic of the Cu(I)/Cu(0) system was analysed at all scan rates. The use of (12) and (13) yields average values of the standard rate constant k^0 (cm/s): $4.86 (\pm 0.68) \times 10^{-5}$, $4.63 (\pm 0.22) \times 10^{-5}$, respectively.

TABLE I
KINETIC-MASS TRANSPORT PARAMETERS FOR Cu(I)/Cu(0) REDOX COUPLE

Cu(I)/Cu(0) System	$D_{Cu(I)} [10^{-9} m^2 s^{-1}]$		α	$k^0 [10^{-5} cm s^{-1}]$	
	Semi-integration	Tafel		Kinetic diagrams (12) (13)	
	1.75	0.82		3.835	4.99

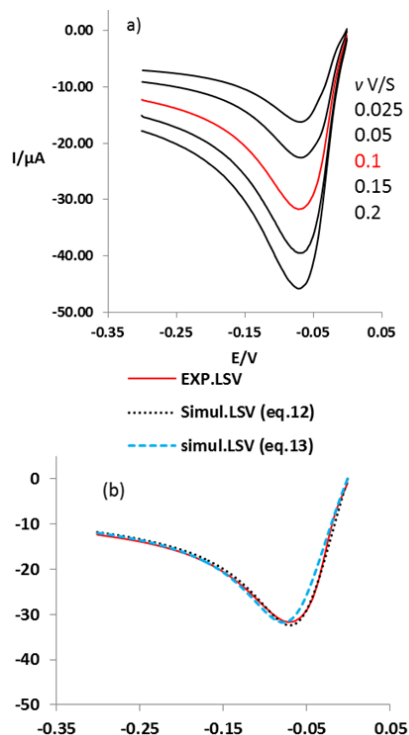


Fig. 5 (a) Typical LSV curves of electrodeposition of Cu(I) on Cu disc electrode from 10.25 mM of tetrakis(acetonitrile)copper(I) tetrafluoroborate in acetonitrile at various scan rates; (b) Comparison of simulated LSV responses with experimental data recorded at 100 mV/S using fit models presented by (12) and (13); parameters used for simulation of linear sweep voltammograms are illustrated in Table I

VI. CONCLUSION

LSV responses were first calculated under reversible, quasi and irreversible conditions using the well-known method of Nicholson, the semi analytical method. After that, series of Kinetic zone diagrams illustrating the different observable voltammetric behaviors as a function of both kinetic rate constant and charge transfer coefficient were established and presented in this paper. Fitting these diagrams leads to general models that permit to experimenter to estimate easily the kinetic parameters whatever the degree of reversibility. Our LSV models are tested and gave a good agreement.

NOMENCLATURE

C_M	Concentration of the metal M
$C_{M^{n+}}$	Concentration of the metallic ions Mn^{+}
$D_{M^{n+}}$	Diffusion coefficient of metallic ions Mn^{+}
A	Electroactive surface area
F	Faraday's constant
R	Universal gas constant
T	Absolute temperature
k^0	Standard rate constant
I	Current

$E(t)$	Electrode potential
E_i	Initial potential
E^0	Standard potential
α	Charge transfer coefficient
$1-\alpha$	Anodic charge transfer coefficient
Ψ	Dimensionless current
η	Dimensionless overvoltage : $\eta = nF / RT (E - E_{eq})$

REFERENCES

- [1] L.K. Bieniasz, Analysis of the applicability of the integral equation method in the theory of transient electroanalytical experiments for homogeneous reaction-diffusion systems: The case of planar electrodes, *J. Electroanal. Chem.* 657 (2011) 91–97. doi:10.1016/J.JELECHEM.2011.03.027
- [2] L.K. Bieniasz, Use of dynamically adaptive grid techniques for the solution of electrochemical kinetic equations: Part 5. A finite-difference, adaptive space/time grid strategy based on a patch-type local uniform spatial grid refinement, for kinetic models in one-dimensional space geometry, *J. Electroanal. Chem.* 481 (2000) 115–133. doi:10.1016/S0022-0728(99)00460-X.
- [3] D. Yan, M.Z. Bazant, P.M. Biesheuvel, M.C. Pugh, F.P. Dawson, Theory of linear sweep voltammetry with diffuse charge: Unsupported electrolytes, thin films, and leaky membranes, *Phys. Rev. E* 95 (2017) 33303. doi:10.1103/PhysRevE.95.033303
- [4] K.B. Oldham, J.C. Myland, Modelling cyclic voltammetry without digital simulation, *Electrochim. Acta.* 56 (2011) 10612–10625. doi:10.1016/J.ELECTACTA.2011.05.044. W.-K. Chen, *Linear Networks and Systems* (Book style). Belmont, CA: Wadsworth, 1993, pp. 123–135.
- [5] D. Krulic, N. Fatouros, D. Liu, A complementary survey of staircase voltammetry with metal ion deposition on macroelectrodes, *J. Electroanal. Chem.* 754 (2015) 30–39. doi:10.1016/J.JELECHEM.2015.06.012.
- [6] A. Saila, Etude des systemes electrochimiques quasi-reversibles par voltamperometrie a balayage lineaire et semi-integration. Applications aux comportements de rhenium et dysprosium en milieux de sels fondus, Univ. Badji Mokhtar, Annaba, 2010. <http://biblio.univ-annaba.dz/wp-content/uploads/2015/01/SAILA-Abdelkader.pdf>.
- [7] I. Atek, S. Maye, H.H. Girault, A.M. Affoune, P. Peljo, *J. Electroanal. Chem.* 818 (2018) 35–43.
- [8] T. Berzins, P. Delahay, Oscillographic Polarographic Waves for the Reversible Deposition of Metals on Solid Electrodes, *J. Am. Chem. Soc.* 75 (1953) 555–559. doi:10.1021/ja01099a013.
- [9] H. Matsuda, Y. Ayabe, Zur Theorie der Randles-Sevcik'schen Kathodenstrahl-Polarographie, *Zeitschrift Für Elektrochemie, Berichte Der Bunsengesellschaft Für Phys. Chemie.* 59 (1955) 494–503. doi:10.1002/BBPC.19550590605.
- [10] P. Peljo, D. Lloyd, N. Doan, M. Majaneva, K. Kontturi, Towards a thermally regenerative all-copper redox flow battery, *Phys. Chem. Chem. Phys.* 16 (2014) 2831–2835. doi:10.1039/C3CP54585G.
- [11] R.R. Bessette, J.W. Olver, Measurement of diffusion coefficients for the reduction of copper(I) and (II) in acetonitrile, *J. Electroanal. Chem.* 21 (1969) 525–529. doi:10.1016/S0022-0728(69)80329-3.